Virology Journal

RESEARCH

Open Access

Immune evasion, infectivity, and membrane fusion of the SARS-CoV-2 JN.1 variant

Haijun Tang[1,2†], Yanhang Zhuo[1,2†], Jianlin Chen[1,3†], Rongzhao Zhang[1,2†], Miao Zheng[4], Xinghua Huang[1,2], Yisheng Chen[1,2], Minjian Huang[1,2], Zhaonan Zeng[1,2], Xueping Huang[5,6*], Chenfeng Han[7*] and Yi Huang[1,2,3,8,9*]

Abstract

SARS-CoV-2 undergoes continuous mutations during transmission, resulting in a variety of Omicron subvariants. Currently, SARS-CoV-2 BA.2.86 and its descendants JN.1, KP.2, KP.1.1 have been identified as the primary variants spreading globally. These emerging Omicron variants have increased transmissibility, potentially elevating the risk of viral reinfection in the population. However, the biological characteristics of newly-emerged Omicron subvariants in infecting host cells remain unclear. In this study, we assessed the neutralization effect of BA.2.86 and its descendant JN.1, as well as D614G, BA.2, BA.4/5, XBB.1.5, EG.5.1, HV.1, HK.3, JD.1.1 and JG.3 on convalescent sera obtained from individuals infected with BA.5 or XBB.1.5 strain. We evaluated the biological characteristics of variants spike proteins by measuring viral infectivity, affinity for receptors, and membrane fusion. Compared to XBB-related subvariants, BA.2.86 exhibited a diminished immune escape response, but JN.1 displayed a markedly augmented immune escape capability, which was closely related to its rapid transmission. BA.2.86 was less infectious in susceptible cells, while the JN.1 variant exhibited relatively high infectivity. Notably, BA.2.86 and JN.1 exhibited low fusion activity in 293 T-ACE2 cells, but relatively high fusogenicity in transmembrane protease serine 2 (TMPRSS2) overexpression cells. This study explored the evolutionary characteristics of emerging Omicron subvariants in host adaptation, and provided new strategies for the prevention and treatment of coronavirus disease 2019 (COVID-19).

Keywords Omicron subvariant, JN.1, Immune escape, Infectivity

†Haijun Tang, Yanhang Zhuo, Jianlin Chen and Rongzhao Zhang contributed equally to this work.

*Correspondence:
Xueping Huang
hxuep@mail2.sysu.edu.cn
Chenfeng Han
hanchenfeng93@163.com
Yi Huang
hyi8070@126.com
[1] Shengli Clinical Medical College, Fujian Medical University, Fuzhou, Fujian 350001, China
[2] Center for Experimental Research in Clinical Medicine, Fujian Provincial Hospital, Fuzhou, Fujian 350001, China
[3] Department of Clinical Laboratory, Fujian Provincial Hospital, Fuzhou, Fujian 350001, China
[4] College of Integrative Medicine, Fujian University of Traditional Chinese Medicine, Fuzhou, Fujian 350001, China
[5] Department of Gastroenterology, Shengli Clinical Medical College of Fujian Medical University, Fuzhou 350001, Fujian, China
[6] Department of Gastroenterology, Fujian Provincial Hospital, Fuzhou, Fujian 350001, China
[7] Department of Blood Transfusion, The First Affiliated Hospital of Soochow University, Suzhou, Jiangsu Province 215000, China
[8] Central Laboratory, Fujian Provincial Hospital, Fuzhou, Fujian 350001, China
[9] Fujian Provincial Key Laboratory of Cardiovascular Disease, Fujian Provincial Key Laboratory of Critical Care Medicine, Fuzhou, Fujian 350001, China

Introduction

SARS-CoV-2 is constantly mutating during transmission, posing a serious threat to human health [1, 2]. In particular, following the emergence of the Omicron BA.1 variant, the evolution rate of the virus was accelerated significantly, and a large number of new Omicron subvariants continued to emerge, replacing the previous main circulating strains [3, 4]. Currently, SARS-CoV-2 BA.2.86 and its descendants JN.1, KP.2, KP.1.1 have become the major epidemic strains in the world [2, 5, 6]. Compared with BA.2 strain, BA.2.86 and its descendants carry more than 30 additional mutations in the viral spike protein [7, 8]. JN.1 possesses an extra mutation, L455S, in the spike protein, while KP.2 has two mutations, F456L and R346T. Previous studies have shown that Omicron variants harbor the L455F mutation, which contributes to increased viral transmission and immune escape [2, 9, 10]. Emerging mutations in the spike protein of the variant may enhance the transmissibility of the virus and increase the risk of viral reinfection in the human population.

The ability of SARS-CoV-2 to infect target cells is related to the cleavage activity of Furin protease on spike protein and the binding affinity between spike protein and receptor. Previous research has indicated that the Delta variant carries a P681R mutation, enhancing its ability to infect cells that express high levels of transmembrane serine protease [11]. Nevertheless, the Furin protease's cleavage activity was diminished by the P681H mutation in the Omicron variant, increasing the virus's propensity to infect host cells via the endocytic pathway [11, 12]. Mutations in the viral spike protein may alter its conformation, affecting its interaction with the host receptor ACE2. Certain spike protein mutations may enhance cross-species transmission by bolstering its binding affinity for the non-human species receptor ACE2 [13, 14]. The large number of mutations in the spike proteins of BA.2.86 and JN.1 distinguishes it from other circulating Omicron variants. In particular, the P681R mutation in the S1/S2 cleavage site of the BA.2.86 and JN.1 spike proteins may affect viral fusogenicity. However, compared to the previous dominant SARS-CoV-2 Omicron variant, JN.1 has not been systematically evaluated for its fusogenicity and ability to infect target cells.

SARS-CoV-2 spike proteins serve as primary targets for neutralizing antibodies generated by natural infection or vaccination [1, 3, 15]. However, spike protein mutations in variants may alter the antigenicity of the virus, diminishing vaccine effectiveness and potentially increasing susceptibility to reinfection [3, 16]. The widespread mutations in SARS-CoV-2 BA.2.86 and its descendants have raised concern about its ability to escape antibody neutralization. Recent evidence indicates that BA.5 breakthrough infection significantly diminishes the diversity of neutralizing antibody epitopes, while increasing the proportion of non-neutralizing mAbs [17]. This implies that the humoral immunity triggered by Omicron breakthrough infection may be less effective against newly emerging Omicron subvariants. Furthermore, the gradual decline of antibody levels in vivo underscores the urgency to understand the impact of Omicron breakthrough infections on neutralization effectiveness against prevalent variants. Recent studies have shown that the BA.2.86 strain does not have a stronger immune escape ability than the XBB strain [18–20]. Therefore, it is critical to understand whether current COVID-19 patients are still able to produce antibodies that effectively neutralize JN.1 and its offspring strains. In addition, it is unclear whether the JN.1 strain may exhibit a growth advantage over other circulating Omicron variants, including BA.2.86 and XBB-related subvariants. In this study, we characterized the biological characteristics of JN.1 by investigating its cross-species infection ability, binding ability to ACE2, membrane fusogenicity, viral entry pathway, and immune evasion capacity compared to other SARS-CoV-2 variants.

Materials and methods

Serum samples

Human sera were collected from individuals who received three doses of inactivated vaccine (CoronaVac and/or BBIBP-CorV, 1 month), Omicron BA.5 breakthrough infection (1 month or 4 months), or Omicron BA.5 + XBB.1.5 breakthrough infection (1 month). Experiments related to SARS-CoV-2 were conducted following the research protocol approved by the Ethics Committee of Fujian Provincial Hospital (number: K2023-03–011). All participants provided written informed consent for the collection of information, storage and use of clinical samples for research purposes, and publication of the data generated in this study.

Cell lines

293T, Vero, Huh7, Caco-2, and A549 cells were obtained from American Type Culture Collection. The human lung adenocarcinoma cell line Calu-3 was purchased from Pricella. 293T-ACE2, Caco2-ACE2, A549-ACE2, and 293T-ACE2-TMPRSS2 cells were generated by lentivirus-mediated gene transduction. Wild-type 293T cells exhibit negligible endogenous ACE2 expression. The 293T-ACE2 cells produced by exogenous gene transfection eliminated the interference of natural receptor expression. SARS-CoV-2 enters target cells mainly through endocytosis, but can also directly invade host cells through cell surface serine protease-mediated cleavage of the spike protein. The study of SARS-CoV-2 infection using

293T-ACE2-TMPRSS2 cells can clarify the dependence of the virus on TMPRSS2. The Calu-3 human lung adenocarcinoma cell line endogenously expresses ACE2 and TMPRSS2 at physiological levels, which can be used as a biologically model for studying SARS-CoV-2 pulmonary infection. All cell lines were cultured in DMEM (Gibco) supplemented with 1% penicillin–streptomycin (Gibco) and 10% fetal bovine serum (Gibco).

Production of SARS-CoV-2 variants pseudoviruses

The pcDNA3.1 plasmids encoding SARS-CoV-2 variants spike protein were generated by Genscript Biotechnology. Pseudoviruses were generated by replacing viral glycoproteins with SARS-CoV-2 variant spike proteins in the background of vesicular stomatitis virus (VSV) according to methods reported in our previous study [21]. The backbone of the pseudovirus is derived from the VSV virus, with the G gene replaced by firefly luciferase and the eGFP reporter gene, and the SARS-CoV-2 spike protein incorporated as a membrane protein on the surface of the VSV pseudovirus. However, pseudoviruses are replication-deficient, as they lack the ability to express surface proteins or form complete viral particles. Therefore, pseudoviruses cannot replicate continuously and can only carry out a single round of infection. Pseudovirus infection mainly reflects the process of virus entry into host cells. Briefly, 293 T cells were seeded in 10 cm dishes and cultured overnight in a 5% CO_2 humidified incubator prior to plasmid transfection. The next day, when cell density reached 80–90% confluence, 293 T cells were transfected with spike protein-expressing plasmids using Lipofectamine 3000 (Invitrogen). 12 h after transfection, cells were challenged with G*ΔG-VSV pseudotyped particles bearing both firefly luciferase and eGFP reporter genes. After 6 h of incubation, the cell culture supernatant was discarded and the cells were gently washed twice with phosphate-buffered saline (PBS). Subsequently, 10 mL of fresh DMEM was replenished to the culture dish. At 24 h post-infection, pseudovirus-containing supernatants were collected, centrifuged at 3,500 g for 5 min to remove cellular debris, and stored at -80°C. Target cells were infected with G*ΔG-VSV pseudoviral particles packaged with empty vector as the baseline level of viral infection.

To verify whether SARS-CoV-2 variant pseudoviruses were successfully packaged, 293T cells (lacking ACE2) and 293T-ACE2 cells were infected with pseudoviruses. After incubation for 24 h, GFP expression was observed under an inverted fluorescence microscope. Meanwhile, luciferase activity in cell lysates was measured to determine the viral infection efficiency. Pseudovirus particles were quantified by RT-qPCR according to our previously reported method [21]. The viral titer was determined by 50% tissue culture infectious dose (TCID50) in 293T-ACE2 cells. Viral supernatants were serially diluted tenfold in DMEM, inoculated into cells, and incubated at 37°C for 48 h. GFP expression was then visualized under a fluorescence microscope. TCID50 per ml was calculated using the Karber method.

Pseudovirus infection assay

Prior to pseudovirus infection assays, we normalized viral particles to the same amount using quantitative RT-PCR (qRT-PCR). To evaluate spike protein-mediated cell entry, target cells (3×10^4/well) were seeded in 96-well plates one day before viral infection. The next day, cell culture medium was discarded and cells were inoculated with 100 μL of pseudovirus-containing medium. At 24 h post-infection, cells were lysed with 60 μL of diluted passive lysis buffer (Promega) for 10 min at room temperature. Subsequently, cell lysates were mixed with luciferase substrate (Promega) and measured using a SpectraMax L microplate reader (Molecular Devices). Cells infected with VSV pseudovirus (G*ΔG-VSV) packaged with empty vector served as negative control. Variant pseudovirus infection data were background-corrected by subtracting negative control values from raw measurements, while SARS-CoV-2 D614G was included as positive control.

The pLVEF1αIHRB vectors (containing H2BmRuby3 reporter gene) carrying the ACE2 gene of different species were kindly provided by Prof. Tong Cheng (Xiamen University, China) [22]. To investigate the cross-species transmission potential of Omicron subvariants, we transfected pLVEF1αIHRB vectors containing ACE2 genes of different species into 293 T cells. After 24 h, the cells were digested and seeded in 96-well plates with 3×10^4 cells per well and then cultured for another 24 h before pseudovirus infection. 293 T cells transfected with empty vector were used as control.

SARS-CoV-2 live virus infection assay

SARS-CoV-2 JN.1, EG.5.1 and HK.3 variants were isolated from laboratory-confirmed COVID-19 patients at the First Affiliated Hospital of Zhejiang University. All SARS-CoV-2 variants were cultured and expanded in Vero cells. The collected viral supernatants were serially diluted tenfold in DMEM medium, and the infective dose was determined by TCID50. The experiments were conducted in the Biosafety Level 3 (BSL-3) facility of the First Affiliated Hospital of Zhejiang University.

293T-ACE2, 293T-ACE2-TMPRSS2 and Calu-3 cells were prepared in 12-well plates and infected with JN.1, EG.5.1, and HK.3 in 1 mL DMEM at 500 TCID50 for 2 h. The residual inoculum was removed and the cells were washed with PBS and then supplemented with fresh

medium. Cell culture supernatant and cell lysate were collected at 2, 24 and 48 h after virus infection. Viral RNA was extracted from 200 μL of virus-containing supernatant using the QIAamp Viral RNA Mini Kit (QIAGEN). For cell lysates, RNA was extracted using the Super FastPure Cell RNA Isolation Kit (Vazyme). Viral RNA copy number was quantified by RT-qPCR using SARS-CoV-2 Nucleic Acid Detection Kit (Liferiver).

Flow cytometric analysis of ACE2 binding to SARS-CoV-2 variants spike proteins

To assess the binding affinity of ACE2 with SARS-CoV-2 variant spike proteins, we introduced plasmids encoding variant spike proteins into 293T cells using Lipofectamine 3000 [23]. 36 h after transfection, the cells were isolated with EDTA and then washed twice with 1 mL staining buffer. Then, cells were incubated with mouse anti-SARS-CoV-2 spike antibody (Genetex, 1 μg/mL) or soluble recombinant human ACE2-hFc fusion protein (Sino Biological, 1 μg/mL) for 1 h. Next, the cells were incubated with PE-labeled anti-mouse IgG (Biolegend) or PE-labeled anti-human IgG Fc (Biolegend) secondary antibodies. After final washing, cells were resuspended in staining buffer and analyzed by flow cytometer Accuri C6 (BD Biosciences, USA). 293T cells transfected with empty plasmids and stained were used as negative controls. Binding activity was determined by mean fluorescence intensity (MFI) and normalized by cell surface expression of spike proteins (sACE2/S2).

Effect of endocytosis or protease inhibitors on Omicron variants pseudovirus infection

293T-ACE2 or 293T-ACE2-TMPRSS2 cells (3×10^4 cells) were seeded in 96-well plates one day before virus infection. The next day, target cells were pretreated with different doses of inhibitors or DMSO for 2 h prior to virus infection. Subsequently, SARS-CoV-2 variants pseudoviruses were used to infect target cells. 24 h after virus infection, virus infection efficiency was quantified by measuring luciferase activity in cell lysates.

Cell–cell fusion assay

To detect cell–cell fusion mediated by ACE2 and variant S proteins, we constructed a T7 polymerase mediated reporter system. This reporter system includes expression vectors for T7 promoter-IRES-Luc2 (T7 pro) and T7 polymerase-T2A-EGFP (T7 pol). 293T cells (donor) were transfected with variants spike, T7 pro and pRL-TK expression plasmids, while 293 T-ACE2 or 293 T-ACE2-TMPRSS2 cells (acceptor) were transfected with T7 pol expression plasmids. After 36 h of transfection, cells were resuspended at 2×10^6/mL, and then donor and acceptor cells were mixed at a 2:1 ratio. Cells were cultured for 12 to 16 h at 37°C, syncytic images were captured using fluorescence microscopy, and cell lysates were used for dual-reporter luciferase assay (Promega).

Pseudovirus neutralization assay

To test the neutralizing activity of vaccine sera, serial fivefold dilution of samples were prepared with the initial dilution of 1:20 and then incubated with 1000 TCID50 pseudoviruses at 37°C for 1 h. Diluted sera containing SARS-CoV-2 pseudoviruses were incubated at 37°C for 1 h, and viruses without sera served as controls. The mixture was inoculated into 293T-ACE2 cells and incubated at 37°C for 24 h. Sera neutralising activity was assessed by measuring luciferase activity in cell lysates.

Statistical analysis

Statistical analyses were performed using GraphPad Prism 8. Data were presented as mean ± standard deviation (SD). The calculation of half-maximal inhibitory concentration (IC50) or half-maximal inhibitory dilution (ID50) was carried out using the four-parameter dose-inhibition response equation in GraphPad Prism 8. Statistical analysis was performed using two-tailed Student's t-test with Welch correction (viral infectivity, ACE2 binding, cell–cell fusion, and viral entry pathway). Serum neutralising activity against variants pseudoviruses was evaluated using the Wilcoxon paired signed-rank test. Statistical significance was determined by a p-value less than 0.05, with ns representing no significant difference, $^{*}p<0.05$, $^{**}p<0.01$, $^{***}p<0.001$, $^{****}p<0.0001$.

Results

The SARS-CoV-2 JN.1 variant exhibits increased infectivity in susceptible cells

To investigate the biological characteristics of the major circulating SARS-CoV-2 variants, we constructed 11 SARS-CoV-2 variant spike proteins, including D614G, BA.2, BA.4/5, XBB.1.5, EG.5.1, HV.1, HK.3, JD.1.1, JG.3, BA.2.86, and JN.1 (Fig. S1A-B). Among them, D614G, BA.2 and BA.4/5 were the major variants in the early SARS-CoV-2 pandemic. XBB.1.5, HV.1, HK.3, JD.1.1, and JG.3 were the main circulating strains prior to JN.1, and BA.2.86 served as the ancestral lineage of JN.1. We generated each pseudovirus using the VSV pseudovirus system and then assessed their ability to infect different types of target cells. Pseudoviruses harbouring spike proteins from BA.4/5, XBB.1.5, EG.5.1, HV.1, HK.3, JD.1.1, JG.3 and JN.1 showed increased infection efficiency compared to BA.2 (Fig. 1). In 293 T-ACE2, Vero, and A549-ACE2 cells, BA.2.86 exhibited a similar infection to BA.2. The infection capacity of BA.2.86 pseudovirus was slightly enhanced in 293 T-ACE2-TMPRSS2, Caco2-ACE2, Calu-3 and Huh 7 cells. In most tested susceptible cells,

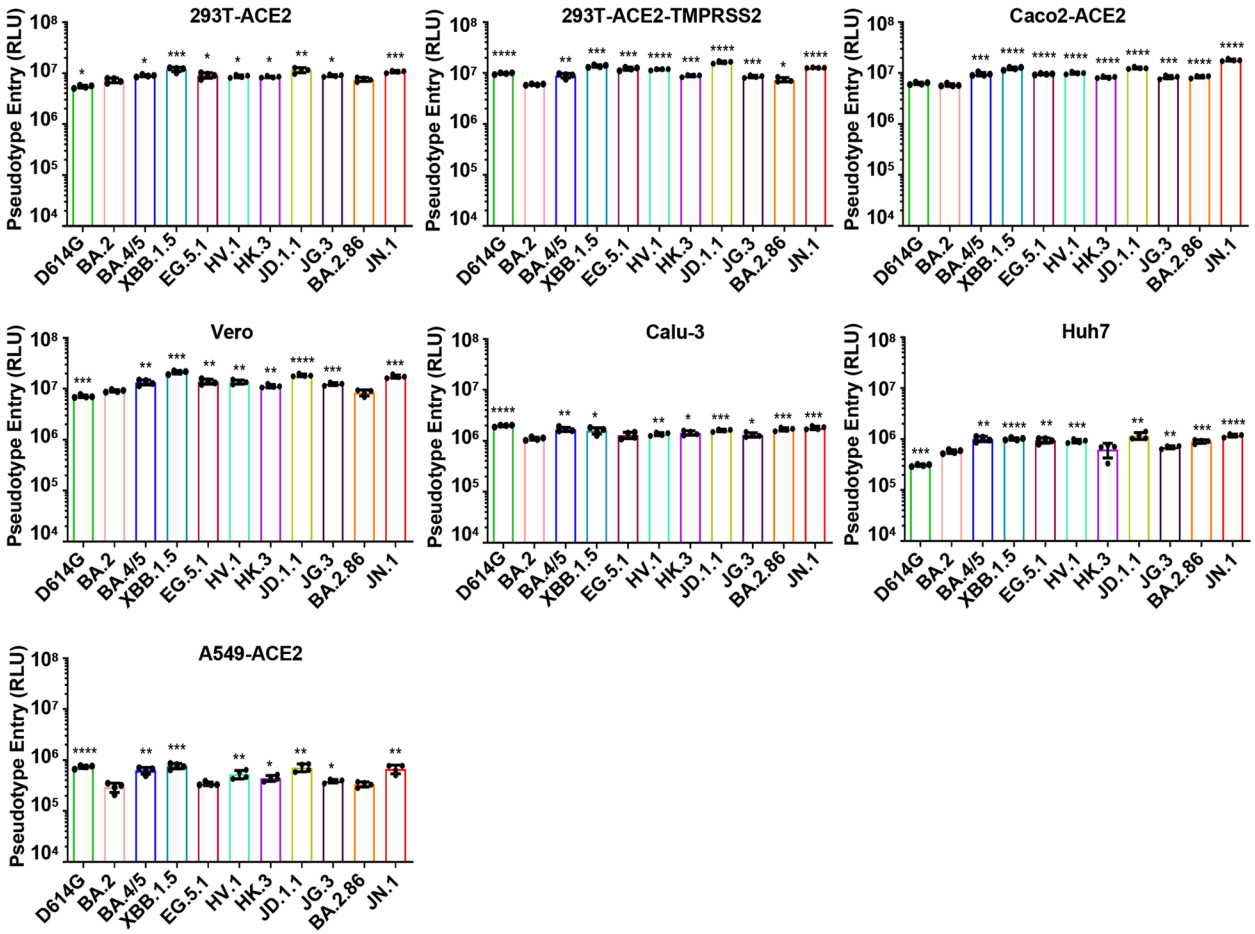

Fig. 1 Infectivity analysis of pseudoviruses carrying SARS-CoV-2 variants spike proteins to susceptible cells. Pseudoviruses bearing SARS-CoV-2 variants spikes of interest were used to infect 293T-ACE2, 293T-ACE2-TMPRSS2, Caco2-ACE2, Vero, Calu-3, Huh7, and A549-ACE2 cells. All statistical comparisons were performed relative to the BA.2 variant. The experiments were conducted with 4 replicates and repeated at least twice. One representative is shown with error bars denoting SD. Statistical analysis was performed using two-tailed Student's t-tests; *$p < 0.05$, **$p < 0.01$, ***$p < 0.001$, ****$p < 0.0001$. RLU, relative luminescence units

JN.1 exhibited higher infectivity than other SARS-CoV-2 variants, with the exception of XBB.1.5 and JD.1.1, which showed similar infection capability to JN.1. Furthermore, in Calu-3 and A549-ACE2 cell lines, the D614G variant exhibited infection efficiency comparable to JN.1. Notably, JN.1 exhibited higher infectivity than BA.2.86 in most of the susceptible cells, indicating its rapid spread capability.

JN.1 is more susceptible to cross-species infection than BA.2.86

SARS-CoV-2 recognizes and attaches to the host membrane protein ACE2 through its spike protein to invade host cells [24]. Further, to examine the cross-species transmission potential of dominant Omicron subvariants, we evaluated the infectivity of Omicron subvariants to cells expressing ACE2 homologues of 10 different species. Flow cytometry analysis showed that ACE2 expression levels (by activated red fluorescence of H2BmRuby3) of different species were comparable in 293T cells, indicating consistency in plasmid transduction efficiency (Fig. S2). All the tested SARS-CoV-2 Omicron subvariants could effectively infect cells expressing ACE2 of different species, but their infection efficiency varied significantly (Fig. 2A-B). SARS-CoV-2 BA.4/5, XBB.1.5, EG.5.1, HV.1, HK.3, JD.1.1, JG.3, and JN.1 subvariants had higher infection ability to target cells than BA.2. D614G was less capable of infecting target cells than BA.2 in cells expressing human, camel, mouse, rat, and cat ACE2. However, D614G infection was more potent than BA.2 in cells expressing horse and ferret ACE2. Overall, the Omicron subvariants were more susceptible to 293T cells expressing human, camel, and pig ACE2 than ferret. In addition, pseudoviruses carrying D614G, BA.2, and BA.286 spike proteins were less infectious in cells expressing horse, mouse, rat, and cat

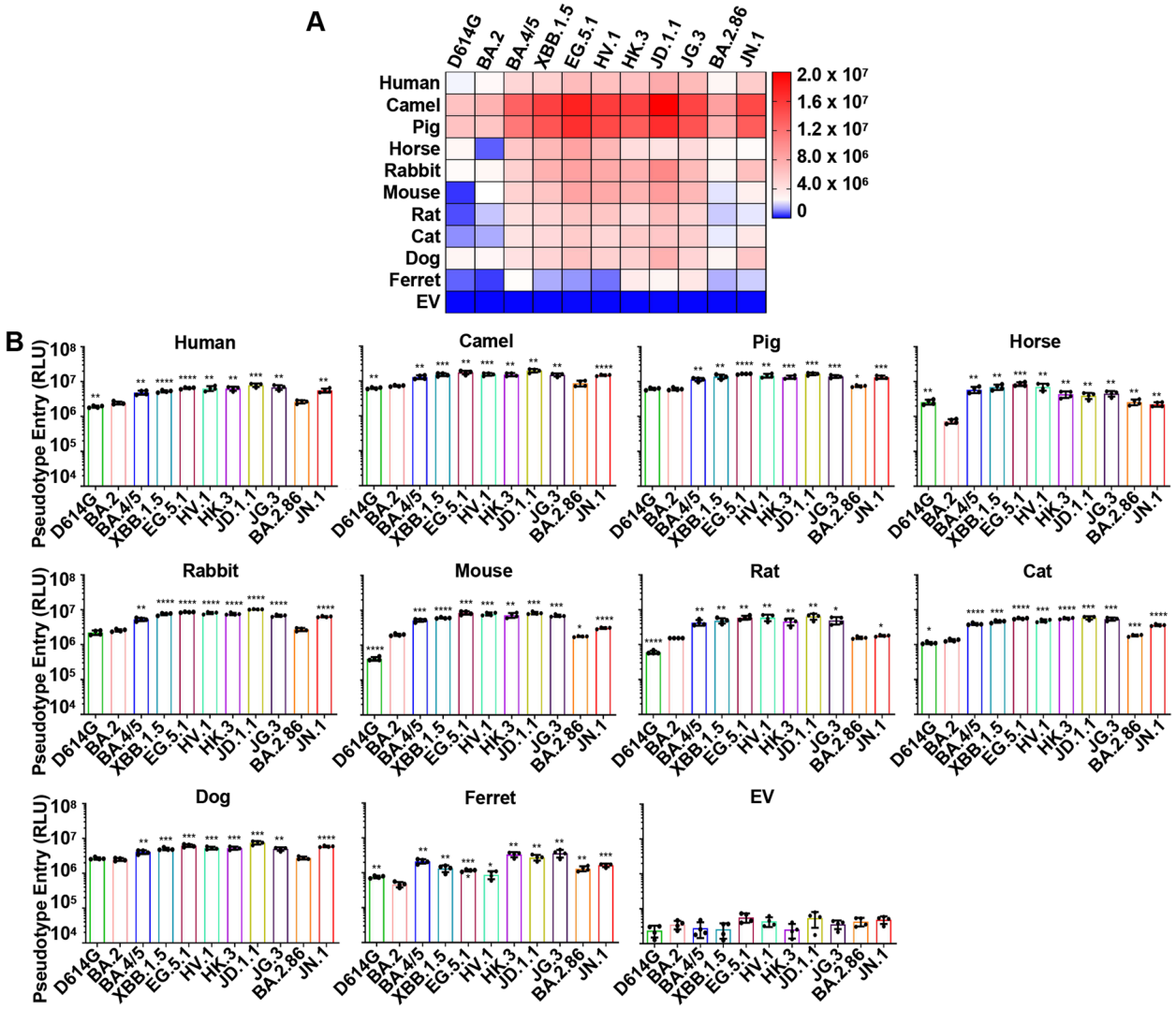

Fig. 2 Cross-species infection potential of emerging Omicron variants. **A** Heat map shows the cross-species infection performance of Omicron pseudoviruses in 293T cells expressing homologous ACE2 from different species. **B** The infective ability of newly emerging Omicron subvariants to 293T cells expressing ACE2 of different species. All statistical comparisons were performed relative to the BA.2 variant. The experiments were conducted with 4 replicates and repeated at least twice. One representative is shown with error bars denoting SD. Statistical analysis was performed using two-tailed Student's t-tests; *$p < 0.05$, **$p < 0.01$, ***$p < 0.001$, ****$p < 0.0001$. EV indicates empty vector

ACE2. Moreover, the infectivity of JN.1 strain was higher than that of BA.2.86 in most ACE2-expressing cells of different species. These findings indicate that emerging Omicron subvariants have a tendency to acquire higher cellular infectivity in different species.

Authentic JN.1 virus entered target cells more efficiently than EG.5.1 and HK.3

To realistically reflect the variation of different strains during infection, we compared the infectivity of some authentic Omicron subvariants in a BSL-3 facility. We evaluated the entry and replication of SARS-CoV-2 JN.1 in 293T-ACE2, 293T-ACE2-TMPRSS2 and Calu-3 cells, with EG.5.1 and HK.3 as comparison groups. Consistent with our findings regarding SARS-CoV-2 variant pseudoviruses entering different cells. The entry of SARS-CoV-2 JN.1 into target cells was more efficient than that of EG.5.1 and HK.3 (Fig. 3A). However, SARS-CoV-2 EG.5.1 and HK.3 were more efficient in replication (Fig. 3B) and viral release (Fig. 3C) in susceptible cells.

Omicron variants maintain relatively high receptor affinity

SARS-CoV-2 binding to the host receptor ACE2 via the spike protein is the key step for virus infection. To

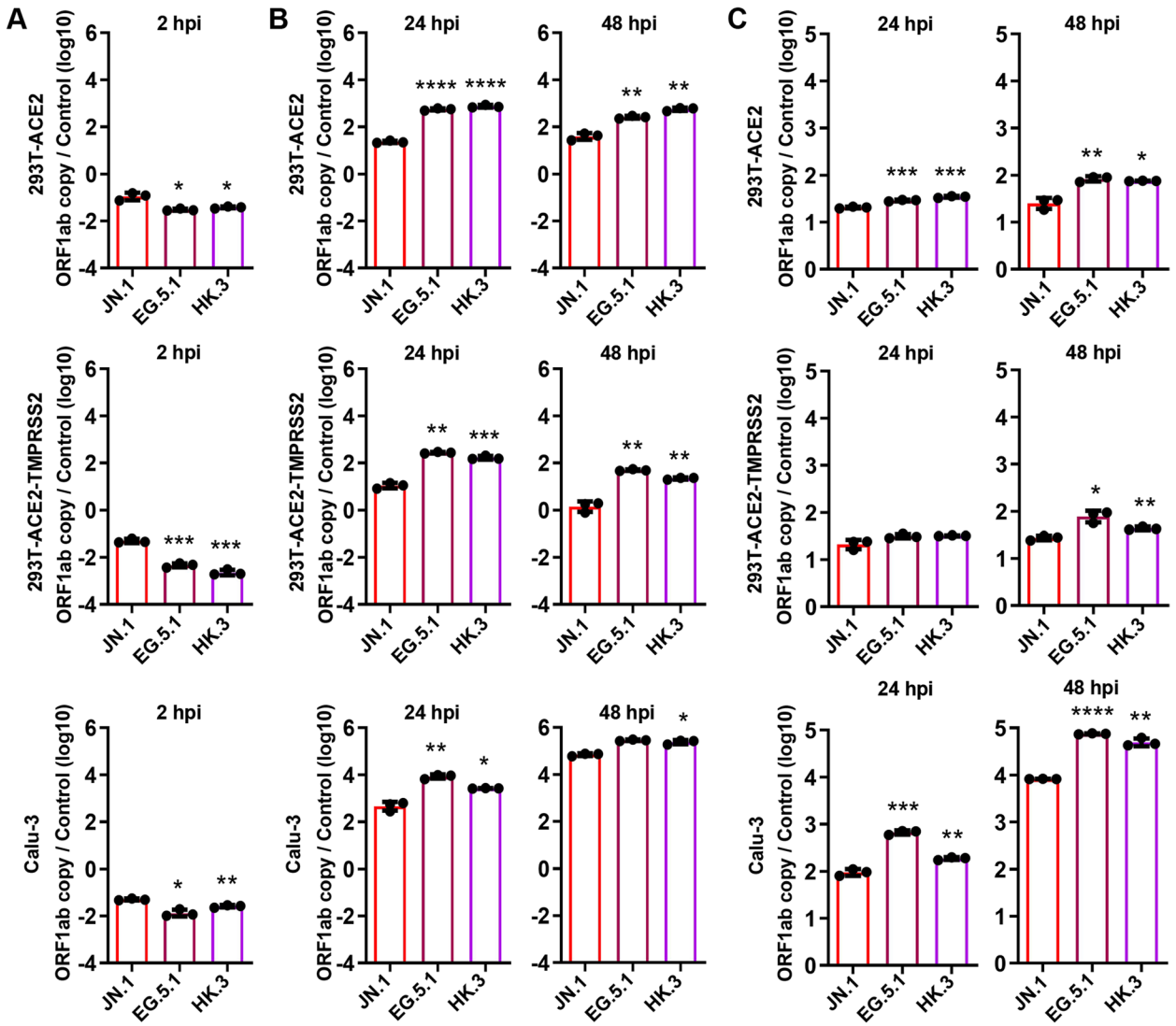

Fig. 3 Entry and replication of authentic SARS-CoV-2 virus in susceptible cells. **A** Entry of authentic SARS-CoV-2 JN.1, EG.5.1 and HK.3 into 293T-ACE2, 293T-ACE2-TMPRSS2, and Calu-3 cells. Cell lysates were quantified for viral ORF1ab gene copies. **B** Replication of authentic SARS-CoV-2 JN.1, EG.5.1 and HK.3 in 293T-ACE2, 293T-ACE2-TMPRSS2, and Calu-3 cells. **C** Release of authentic SARS-CoV-2 JN.1, EG.5.1 and HK.3 in 293T-ACE2, 293T-ACE2-TMPRSS2, and Calu-3 cells. All statistical comparisons were performed relative to the JN.1 variant. The experiments were performed once with 3 replicates. Statistical analysis was performed using two-tailed Student's t-tests; *$p < 0.05$, **$p < 0.01$, ***$p < 0.001$, ****$p < 0.0001$. hpi, hours post infection

clarify the effect of spike protein mutations on SARS-CoV-2 infectivity, we used flow cytometry to assess the binding efficiency of variant spike proteins to soluble recombinant ACE2. Our analysis revealed that Omicron subvariants spike proteins exhibit superior binding affinity to human ACE2 compared to the D614G variant (Fig. 4A-B). While the spike proteins of BA.4/5 displayed binding affinities to human ACE2 comparable to BA.2. The binding efficiencies of XBB.1.5, EG.5.1, HV.1, HK.3, JD.1.1, JG.3, BA.2.86, and JN.1 were markedly higher, which may be a crucial factor in the increased transmissibility of these variants within human populations. Some studies [2, 9] have shown that the binding affinity of the JN.1 receptor binding domain (RBD) to ACE2 is significantly lower than that of BA.2.86. However, we found that the binding affinity of JN.1 full-length spike protein to ACE2 was only slightly lower than BA.2.86. These results suggest that non-RBD of spike proteins also plays a key role in the binding of spike proteins to ACE2.

Fusogenicity mediated by BA.2.86 and JN.1 spike proteins is enhanced in cells overexpressing TMPRSS2

To investigate the biological characteristics of these newly emerging Omicron subvariants, we investigated spike protein-mediated fusogenicity. We evaluated the fusogenicity of Omicron spike proteins in 293T-ACE2 and 293T-ACE2-TMPRSS2 cells. Consistent with previous studies, all Omicron variants tested showed reduced syncytium formation compared to D614G (Fig. 5A-B). When 293T and 293T-ACE2 cells were co-cultured, BA.2.86 and JN.1 exhibited lower cell–cell fusion activity at levels comparable to the ancestral BA.2. However, BA.4/5, XBB.1.5, EG.5.1, HV.1, HK.3, JD.1.1 and JG.3 showed significantly higher fusion activity. Notably, the fusion activity of BA.2.86 and JN.1 was significantly enhanced when 293 T and 293 T-ACE2-TMPRSS2 cells were co-cultured. BA.2.86 and JN.1 exhibited enhanced fusion activity in cells overexpressing TMPRSS2, potentially leading to higher viral infection efficiency.

The JN.1 variant tends to entry into host cells via TMPRSS2-dependent membrane fusion pathway

SARS-CoV-2 binds to the host ACE2 receptor and then fully activates the spike protein to mediate virus entry into target cells via TMPRSS2 on the cell surface or cathepsins in the endosomes [25, 26]. Next, we investigated the entry pathways of Omicron variants pseudoviruses in 293T-ACE2-TMPRSS2 cells in the presence of Camostat (a TMPRSS2 inhibitor) or E64d (an inhibitor of cathepsins). As shown in Fig. 6A, SARS-CoV-2 D614G variant mainly relied on TMPRSS2 to enter host cells, while most Omicron variants were more dependent the endocytic pathway. Similar to the D614G variant, JN.1 preferentially selects TMPRSS2 for entry into host cells. This preference could partially account for the higher cellular infectivity observed with JN.1 compared to BA.2.86. Furthermore, we assessed the impact of endocytosis inhibitors Chloroquine, Apilimod and E64d on the entry of Omicron subvariants into 293T-ACE2 cells. Our results showed that all three inhibitors diminished the entry of variant pseudoviruses into target cells in a dose-dependent manner, with similar efficacy across Omicron subvariants (Fig. 6B). These findings suggest that inhibitors targeting the SARS-CoV-2 entry pathway may offer promising therapeutic potential against emerging Omicron subvariants.

JN.1 exhibits significantly enhanced immune escape compared to BA.2.86

Mutations in SARS-CoV-2 spike proteins may enable the virus to evade immune responses elicited by neutralizing monoclonal antibodies or vaccination [3, 27]. We measured serum neutralizing activity in participants who received three doses of the inactivated SARS-CoV-2 vaccine, as well as in patients with BA.5 or BA.5 + XBB.1.5 breakthrough infection after vaccination. Most individuals vaccinated with inactivated vaccines produced neutralizing antibodies against the BA.5 strain (Fig. S3A). Post-breakthrough infection with BA.5, there was a significant surge in antibody levels, which notably diminished after four months. All XBB-related subvariants, including XBB.1.5, EG.5.1, HV.1, HK.3, JD.1.1, and JG.3, exhibited significantly reduced antibody neutralizing activity compared with D614G, BA.2, and BA.4/5 (Fig. 7A-D, Fig. S3B-C). Similarly, BA.2.86 and JN.1 also displayed decreased antibody neutralizing activity, but BA.2.86 exhibited higher neutralizing activity than XBB-related subvariants. Notably, neutralizing antibody titers against JN.1 were significantly reduced compared with BA.2.86. There was a twofold reduction in ID50 in participants with BA.5 + XBB infection and a 1.2-fold reduction in ID50 in participants with BA.5 infection. This substantial reduction in serum neutralizing activity against newly emerging Omicron subvariants may be a key driver of reinfection with new Omicron strains. Interestingly, we found a marked increase in serum neutralizing activity against Omicron variants among participants who were reinfected with the XBB.1.5 strain after BA.5 infection (Fig. 7C-D). This implies that multiple Omicron infections have the potential to alter the immune imprinting caused by initial vaccination, resulting in the production of powerful neutralizing antibodies against newly emerging Omicron variants.

(See figure on next page.)

Fig. 4 Binding affinities of spike proteins to soluble recombinant ACE2. **A** Binding affinities of newly emerging Omicron variants spike proteins with soluble ACE2, measured by mean fluorescence intensity (MFI) and normalized by cell surface expression of spike proteins (sACE2/S2). All values were weighted by multiplying the number of positive cells in the selected gates. All statistical comparisons were performed relative to the BA.2 variant. The experiments were conducted with 3 replicates and repeated at least twice. One representative is shown with error bars denoting SD. Statistical analysis was performed using two-tailed Student's t-tests; *$p < 0.05$, **$p < 0.01$, ***$p < 0.001$, ****$p < 0.0001$. **B** Flow cytometry plots of the binding affinity of Omicron variants spike proteins to soluble ACE2. 293T cells expressing variants spike proteins were incubated with the indicated Fc-tagged recombinant soluble human ACE2. An anti-Fc (PE) antibody was used to detect Fc-tagged proteins

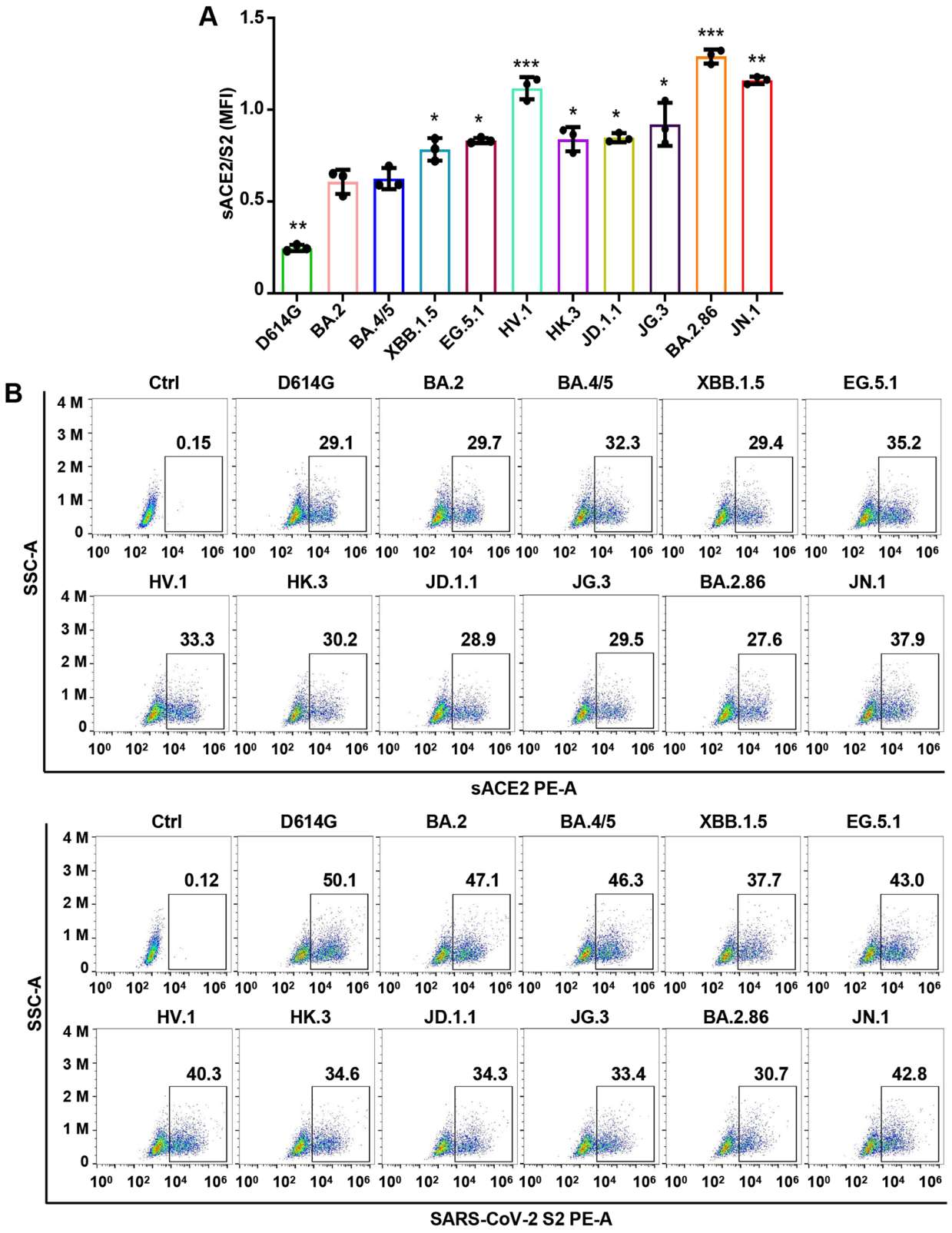

Fig. 4 (See legend on previous page.)

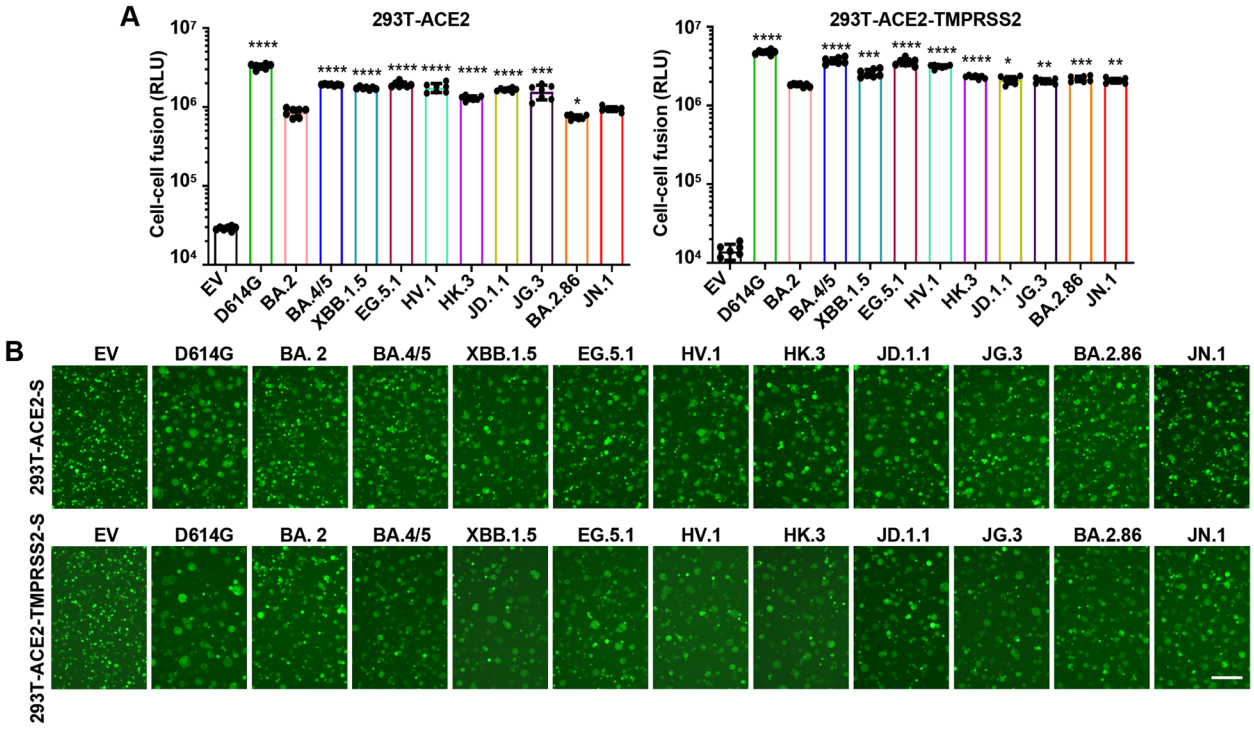

Fig. 5 Fusogenicity mediated by SARS-CoV-2 variants spike proteins in 293T-ACE2 or 293T-ACE2-TMPRSS2 cells. **A** Quantification of cell–cell fusion mediated by ACE2 and variants spike proteins by T7 polymerase reporter system. All statistical comparisons were performed relative to the BA.2 variant. The experiments were conducted with 6 replicates and repeated at least twice. One representative is shown with error bars denoting SD. Statistical analysis was performed using two-tailed Student's t-tests; *$p < 0.05$, **$p < 0.01$, ***$p < 0.001$, ****$p < 0.0001$. EV stands for empty vector. **B** Representative images of cell–cell fusion mediated by SARS-CoV-2 variants spike proteins and ACE2. The scale bar represents 400 μm

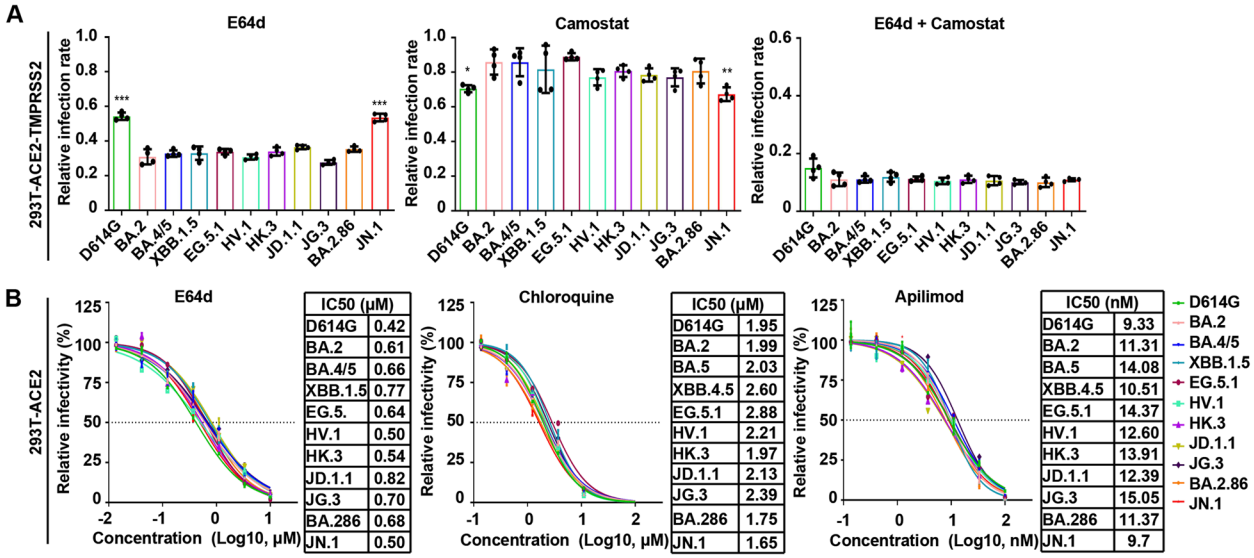

IC50 (μM)	
D614G	0.42
BA.2	0.61
BA.4/5	0.66
XBB.1.5	0.77
EG.5.	0.64
HV.1	0.50
HK.3	0.54
JD.1.1	0.82
JG.3	0.70
BA.286	0.68
JN.1	0.50

IC50 (μM)	
D614G	1.95
BA.2	1.99
BA.5	2.03
XBB.4.5	2.60
EG.5.1	2.88
HV.1	2.21
HK.3	1.97
JD.1.1	2.13
JG.3	2.39
BA.286	1.75
JN.1	1.65

IC50 (nM)	
D614G	9.33
BA.2	11.31
BA.5	14.08
XBB.4.5	10.51
EG.5.1	14.37
HV.1	12.60
HK.3	13.91
JD.1.1	12.39
JG.3	15.05
BA.286	11.37
JN.1	9.7

Fig. 6 Effect of E64d, Camostat, Chloroquine and Apilimod on the entry of pseudoviruses into 293T-ACE2 or 293 T-ACE2-TMPRSS2 cells. **A** Infectivity of variants pseudoviruses in 293T-ACE2-TMPRSS2 cells pretreated with E64d (5 μM) and/or Camostat (50 μM). Asterisks represent statistical differences of SARS-CoV-2 variants compared to the BA.2 strain. The experiments were conducted with 4 replicates and repeated at least twice. One representative is shown with error bars denoting SD. Statistical analysis was performed using two-tailed Student's t-tests; *$p < 0.05$, **$p < 0.01$, ***$p < 0.001$, ****$p < 0.0001$. **B** Effect of E64d, Chloroquine and Apilimod on the entry of pseudoviruses into 293T-ACE2 cells. Experiments were done in 4 replicates and repeated at least twice. One representative is shown with error bars indicating SD

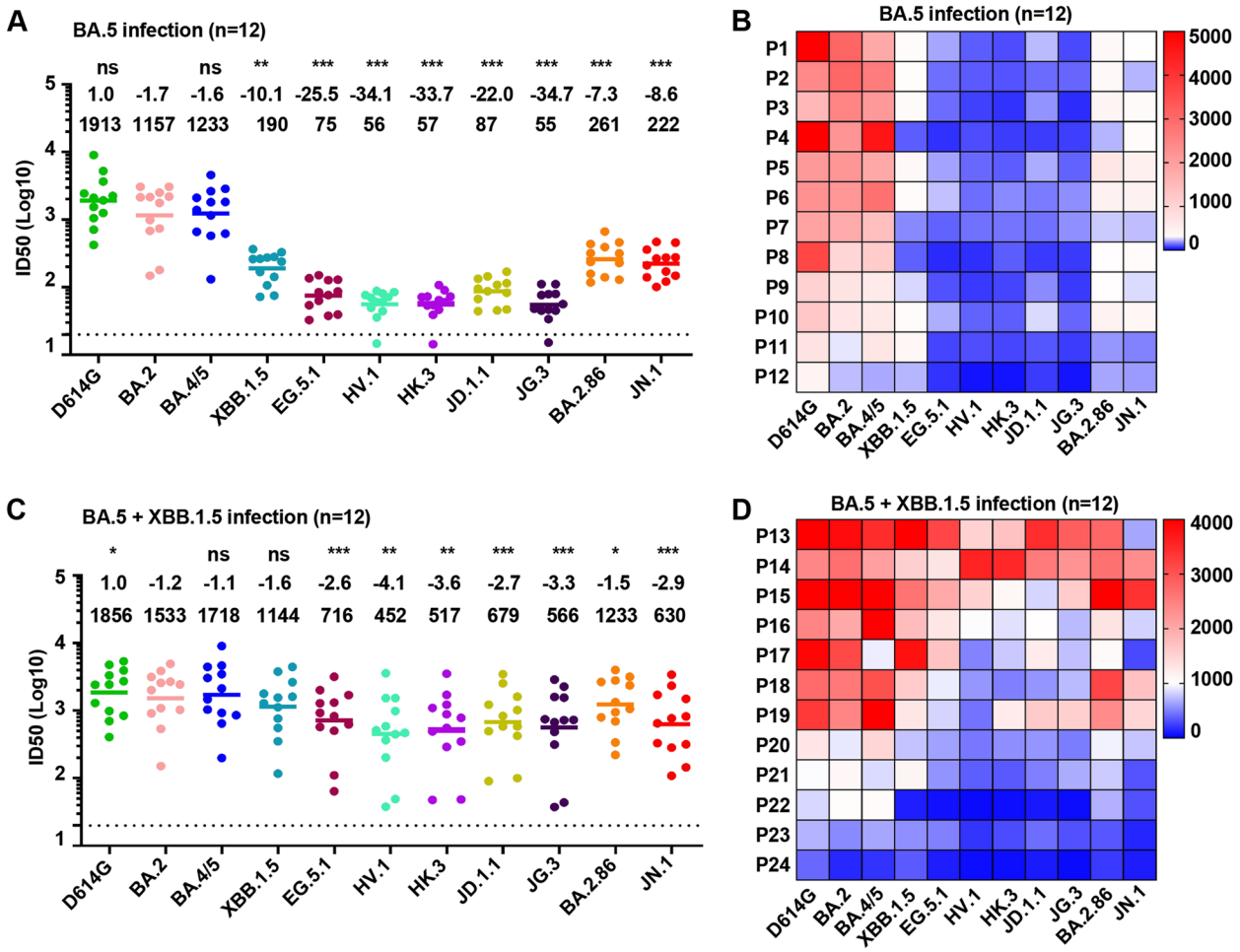

Fig. 7 Neutralizing activity of participants sera against emerging Omicron variants pseudoviruses. **A-B** Neutralizing ID50 titers against Omicron subvariants in convalescent sera from participants with BA.5 breakthrough infections. **C-D** Neutralizing ID50 titers against Omicron subvariants in convalescent sera from participants with BA.5 + XBB.1.5 breakthrough infections. Heatmaps (**B** and **D**) show the ID50 titers of each individual against SARS-CoV-2 variants. The geometric mean titers (GMTs) against each variant are given above the symbols. Fold changes in ID50 titers between Omicron subvariants and D614G are indicated above the GMT labels. P values represent statistical differences for all SARS-CoV-2 subvariants compared to the BA.2 variant. Statistical analysis was performed using Wilcoxon paired signed-rank tests. *$p < 0.05$, **$p < 0.01$, ***$p < 0.001$, ****$p < 0.0001$; ns, not significant. The initial dilutions of serum samples are indicated by dashed lines

Discussion

Viral infectivity and immune resistance are potential risk characteristics of new SARS-CoV-2 variants. Activation of the spike protein by host cell proteases, cleaving the S1/S2 and S2' sites, is essential for membrane fusion and viral entry [28–30]. In TMPRSS2$^-$ cells, the priming of SARS-CoV-2 spike is mediated by the endosomal cysteine protease CatB/L. However, priming of the SARS-CoV-2 spike protein by TMPRSS2 is critical for viral entry into primary target cells and for viral spread in the infected host [29]. Our findings demonstrate that the BA.2.86 variant displayed enhanced infectivity in cells overexpressing TMPRSS2, including 293T-ACE2-TMPRSS2, Caco2-ACE2 and Calu-3 cells, potentially due to heightened fusogenicity mediated by the viral spike protein. Importantly, compared with the BA.2.86 variant, we observed that JN.1 exhibited a considerably increased capacity to infect susceptible cells, consistent with its rapid spread. Previous studies have documented the zoonotic potential of SARS-CoV-2, its transmission from humans to other mammals, which significantly contributes to viral evolution and poses a substantial health risk to humans [13, 22]. Our investigation reveals that mutations in the Omicron spike protein markedly heighten viral infectivity in cells expressing non-human animal ACE2 homologs, especially in species less susceptible to the ancestral strain. This suggests that emerging SARS-CoV-2 variants may

accelerate virus transmission through potential new animal reservoirs.

The binding affinity of SARS-CoV-2 spike protein to ACE2 receptor is a key determinant of viral infectivity, but it is influenced by various factors. For instance, the N501Y mutation in SARS-CoV-2 enhances spike-ACE2 binding affinity, increasing the virus's ability to infect mouse lungs in animal models [31]. Interestingly, high-affinity mutations in the spike protein have been associated with reduced viral infectivity in some contexts [9, 32, 33]. Our research aligns with previous reports on the binding affinity of the circulating Omicron variant spike protein to the ACE2 receptor [3]. We confirmed that circulating Omicron variant spike proteins exhibit higher ACE2 binding affinity than the D614G strain [11]. In particular, XBB.1.5, EG.5.1, HV.1, HK.3, JD.1.1, JG.3, BA.2.86, and JN.1 had stronger binding affinity with the receptor than BA.2 strain. The Omicron variant carries a K417N mutation known to attenuate ACE2 binding, while the N501Y mutation may compensate for this reduction [34, 35]. Furthermore, structural analyses demonstrate that Q493R and Q498R mutations establish new electrostatic interactions with ACE2 residues Glu35 and Asp38, respectively, while the S477N mutation facilitates hydrogen bond formation with ACE2 Ser19 [12, 35]. The synergistic effect of these mutations collectively resulted in a significant increase in the binding affinity of Omicron spike protein to ACE2. Consequently, these results highlight a correlation between the rising infectivity of novel Omicron subvariants and their enhanced affinity to host receptors. Consistent with previous findings [32, 33], we also observed discrepancies between spike-ACE2 binding affinity and pseudoviral infection efficiency in some Omicron variants. Compared with BA.2.86, the binding affinity of JN.1 to human ACE2 was decreased, but its infectivity was significantly higher. We speculate that this divergence is related to the increased efficiency of spike proteolysis by JN.1 spike protein L455S mutation [36].

Previous studies have shown that SARS-CoV-2 spike protein-mediated fusogenicity is closely related to viral infectivity [4, 37, 38]. The spike protein contains a conserved Furin cleavage site at the S1/S2 boundary that regulates proteolytic processing efficiency. In fact, the Delta variant contains the P681R mutation that promotes cleavage of the spike protein and enhances viral fusogenicity, which may account for its enhanced infectivity in cells expressing TMPRSS2 [39, 40]. Omicron carries three characteristic mutations near this Furin cleavage site (P681H, H655Y, and N679K) that collectively reduce S1/S2 cleavage efficiency. This impaired cleavage diminishes TMPRSS2 utilization, leading to suboptimal S2' processing and reduced membrane fusion capacity [12]. Our study shows that the fusion activity mediated by Omicron subvariants spike proteins is significantly weaker than that of D614G. However, the fusion activity of BA.4/5, XBB.1.5, EG.5.1, HV.1, HK.3, JD.1.1, and JG.3 strains was stronger than that of the original BA.2 strain. In addition, the fusion activity of BA.2.86 and JN.1 strains was lower in 293 T-ACE2 cells. Li et al. showed that BA.2.86 and JN.1 variants exhibit enhanced spike protein cleavage efficiency compared with the ancestral BA.2 strain [36]. When evaluated in TMPRSS2 overexpressing cells, both variants exhibit superior membrane fusion capability relative to the BA.2 strain. This biological difference may be due to the spike protein mutations in BA.2.86 and JN.1, specifically the S939F mutation in the HR1 region and the P681R mutation in the S1/S2 cleavage site [39, 41]. Notably, the L455S mutation in the JN.1 spike protein significantly enhances both proteolytic cleavage efficiency and fusogenic activity, thereby augmenting viral infectivity [36, 42]. However, BA.2.86 and JN.1 demonstrated milder pathological manifestations in infected hamsters, which might be associated with their reduced viral replication [42].

Unlike earlier Omicron variants, JN.1 preferentially selects TMPRSS2 for entry into host cells. TMPRSS2 is highly expressed in pulmonary cells but generally shows low expression levels in upper respiratory tract regions such as the trachea [12]. The preference of JN.1 for TMPRSS2 promotes effective infection of TMPRSS2-rich lung cells, suggesting that the virus has an enhanced propensity to infect the lower respiratory tract. The inhibitors Chloroquine, Apilimod and E64d have good blocking effects on all Omicron sublineages. These results suggest that cathepsin inhibitors and endocytosis inhibitors retain inhibitory activity against Omicron variants. Under sustained immune selection pressure, the Omicron variant continues to undergo adaptive evolution, generating novel sublineages with progressively enhanced immune evasion properties. Mutations in the SARS-CoV-2 spike protein enable it to evade antibody neutralization. Nevertheless, viral entry inhibitors maintain antiviral potency as their mechanism of action is independent of immune recognition.

SARS-CoV-2 continues to mutate during transmission, and mutations in spike proteins may evade neutralizing antibodies, thereby compromising the efficacy of COVID-19 vaccines and therapeutic monoclonal antibodies [1, 3, 43]. Emerging Omicron variants carry new immune escape sites and may exhibit a stronger transmission advantage than the parent strains. Post-BA.5 breakthrough infection, there was a notable insufficiency of serum neutralization efficacy against XBB-related subvariants. However, a slight increase in neutralizing antibodies was observed following XBB.1.5 breakthrough

infection. The extensive mutations in the spike protein of BA.2.86 and JN.1 variants raise concerns about evasion of neutralizing antibodies. Previous studies have reported that the increased transmission of BA.2.86 in the human population is mainly caused by enhanced immune evasion [44]. Surprisingly, compared to XBB-related variants, BA.2.86 showed no increase in neutralizing resistance to convalescent sera from BA.5 or XBB.1.5 infected individuals. Nevertheless, BA.2.86 evolved into the JN.1 variant with spike protein L455 mutated into S455, which greatly promoted the evasion of antibody recognition. These results may partly explain why the JN.1 variant has a higher transmission capacity. Taken together, the results indicate that neutralizing antibodies against JN.1 variant induced by BA.5 or XBB.1.5 breakthrough infection remain at low levels. This urgently requires the development of next-generation COVID-19 vaccines against the JN.1 variant and potential future variants.

In conclusion, our study demonstrates that JN.1 exhibits a significantly higher ability to infect susceptible cells compared to the BA.2.86 variant. Authentic virus assays revealed that SARS-CoV-2 JN.1 entered target cells more efficiently than EG.5.1 and HK.3. Additionally, JN.1 showed stronger resistance to convalescent sera from Omicron-infected individuals and exhibited higher immune evasion than BA.2.86. The continuous emergence of new SARS-CoV-2 variants presents a serious public health threat. Our findings underscore the need for the development of vaccines targeting the JN.1 sublineage and other emerging variants to combat the COVID-19 pandemic. Given the ongoing changes in the biological characteristics of new Omicron variants, it is crucial to closely monitor their spread and develop effective therapeutic antibodies and vaccines.

Supplementary Information

The online version contains supplementary material available at https://doi.org/10.1186/s12985-025-02737-3.

Supplementary Material 1.

Acknowledgements
Not applicable.

Authors' contributions
H.T. and Y.Z. performed the experiments and H.T. wrote the manuscript; H.T., J.C. and C.H. analyzed data; R.Z., M.Z., X.H., Y.C., M.H. and Z.Z. contributed to revise the manuscript; C.H., X.H. and Y.H. were responsible for research design, strategy and supervision. All authors have read and approved the article.

Funding
This work was supported by: Joint Fund of Science and Technology Innovation of Fujian Province (2023Y9324); Natural Science Foundation of Fujian Province (2024J011648); Fujian Province Health Care Young and Middle-aged Backbone Talents Training Project (2024GGA001); Medical Vertical Project of Fujian Province (2020CXB001); Joint Fund of Science and Technology Innovation of Fujian Province (2021Y9024); Key Project of Natural Science Foundation of Fujian Province (2022J02048); Provincial Health Commission Major Special Projects (2022ZD01001).

Data availability
No datasets were generated or analysed during the current study.

Declarations

Ethics approval and consent to participate
This study was performed in strict accordance with human subject protection guidance proved by the Research Ethics Committee of Fujian Provincial Hospital (number: K2023-03–011).

Consent for publication
Written informed consent for publication was obtained from the patient.

Competing interests
The authors declare no competing interests.

Received: 19 February 2025 Accepted: 10 April 2025
Published online: 24 May 2025

References

1. Cao Y, et al. BA.2.12.1, BA.4 and BA.5 escape antibodies elicited by Omicron infection. Nature. 2022;608(7923):593–602. https://doi.org/10.1038/s41586-022-04980-y.
2. Yang S, et al. Fast evolution of SARS-CoV-2 BA.2.86 to JN.1 under heavy immune pressure. The Lancet Infectious diseases. 2024;24:e70–2. https://doi.org/10.1016/s1473-3099(23)00744-2.
3. Wang Q, et al. Antibody evasion by SARS-CoV-2 Omicron subvariants BA.2.12.1, BA.4 and BA.5. Nature. 2022;608:603–8. https://doi.org/10.1038/s41586-022-05053-w.
4. Qu P, et al. Immune evasion, infectivity, and fusogenicity of SARS-CoV-2 BA.2.86 and FLip variants. Cell. 2024;187:585-595.e586. https://doi.org/10.1016/j.cell.2023.12.026.
5. Kaku Y, et al. Virological characteristics of the SARS-CoV-2 KP.2 variant. Lancet Infect Dis. 2024;24(7):e416. https://doi.org/10.1016/s1473-3099(24)00298-6.
6. He Q, et al. Neutralization of EG.5, EG.5.1, BA.2.86, and JN.1 by antisera from dimeric receptor-binding domain subunit vaccines and 41 human monoclonal antibodies. Med (New York, NY). 2024;5:401-413.e404. https://doi.org/10.1016/j.medj.2024.03.006.
7. Zhang L, et al. SARS-CoV-2 BA.2.86 enters lung cells and evades neutralizing antibodies with high efficiency. Cell. 2024;187:596-608.e517. https://doi.org/10.1016/j.cell.2023.12.025.
8. Hu Y, et al. Less neutralization evasion of SARS-CoV-2 BA.2.86 than XBB sublineages and CH.1.1. Emerg Microbes Infect. 2023;12:2271089. https://doi.org/10.1080/22221751.2023.2271089.
9. Kaku Y, et al. Virological characteristics of the SARS-CoV-2 JN.1 variant. Lancet Infect Dis. 2024;24:e82. https://doi.org/10.1016/s1473-3099(23)00813-7.
10. Jian F, et al. Convergent evolution of SARS-CoV-2 XBB lineages on receptor-binding domain 455–456 synergistically enhances antibody evasion and ACE2 binding. PLoS Pathog. 2023;19:e1011868. https://doi.org/10.1371/journal.ppat.1011868.
11. Du X, et al. Omicron adopts a different strategy from Delta and other variants to adapt to host. Signal Transduct Target Ther. 2022;7:45. https://doi.org/10.1038/s41392-022-00903-5.
12. Meng B, et al. Altered TMPRSS2 usage by SARS-CoV-2 Omicron impacts infectivity and fusogenicity. Nature. 2022;603:706–14. https://doi.org/10.1038/s41586-022-04474-x.
13. Li L, et al. Broader-species receptor binding and structural bases of Omicron SARS-CoV-2 to both mouse and palm-civet ACE2s. Cell discovery. 2022;8:65. https://doi.org/10.1038/s41421-022-00431-0.

14. Wu L, et al. Broad host range of SARS-CoV-2 and the molecular basis for SARS-CoV-2 binding to cat ACE2. Cell discovery. 2020;6:68. https://doi.org/10.1038/s41421-020-00210-9.
15. Qu P, et al. Evasion of neutralizing antibody responses by the SARS-CoV-2 BA.2.75 variant. Cell Host Microbe. 2022;30:1518-1526.e1514. https://doi.org/10.1016/j.chom.2022.09.015.
16. Faraone JN, et al. Immune evasion and membrane fusion of SARS-CoV-2 XBB subvariants EG.5.1 and XBB.2.3. Emerg Microbes Infect. 2023;12:2270069. https://doi.org/10.1080/22221751.2023.2270069.
17. Cao Y, et al. Imprinted SARS-CoV-2 humoral immunity induces convergent Omicron RBD evolution. Nature. 2023;614:521–9. https://doi.org/10.1038/s41586-022-05644-7.
18. Wang Q, et al. Antigenicity and receptor affinity of SARS-CoV-2 BA.2.86 spike. Nature. 2023;624:639–44. https://doi.org/10.1038/s41586-023-06750-w.
19. Lasrado N, et al. Neutralization escape by SARS-CoV-2 Omicron subvariant BA.2.86. Vaccine. 2023;41:6904–9. https://doi.org/10.1016/j.vaccine.2023.10.051.
20. Khan K, et al. Evolution and neutralization escape of the SARS-CoV-2 BA.2.86 subvariant. Nat Commun. 2023;14:8078. https://doi.org/10.1038/s41467-023-43703-3.
21. Tang H, et al. Multiple SARS-CoV-2 Variants Exhibit Variable Target Cell Infectivity and Ability to Evade Antibody Neutralization. Front Immunol. 2022;13:836232. https://doi.org/10.3389/fimmu.2022.836232.
22. Zhang Y, et al. Cross-species tropism and antigenic landscapes of circulating SARS-CoV-2 variants. Cell Rep. 2022;38:110558. https://doi.org/10.1016/j.celrep.2022.110558.
23. Wang R, et al. Analysis of SARS-CoV-2 variant mutations reveals neutralization escape mechanisms and the ability to use ACE2 receptors from additional species. Immunity. 2021;54:1611-1621.e1615. https://doi.org/10.1016/j.immuni.2021.06.003.
24. Zhou P, et al. A pneumonia outbreak associated with a new coronavirus of probable bat origin. Nature. 2020;579:270–3. https://doi.org/10.1038/s41586-020-2012-7.
25. Jackson CB, Farzan M, Chen B, Choe H. Mechanisms of SARS-CoV-2 entry into cells. Nat Rev Mol Cell Biol. 2022;23:3–20. https://doi.org/10.1038/s41580-021-00418-x.
26. Hui KPY, et al. SARS-CoV-2 Omicron variant replication in human bronchus and lung ex vivo. Nature. 2022;603:715–20. https://doi.org/10.1038/s41586-022-04479-6.
27. Cao Y, et al. BA.2.12.1, BA.4 and BA.5 escape antibodies elicited by Omicron infection. Nature. 2022;608:593–602. https://doi.org/10.1038/s41586-022-04980-y.
28. Ou X, et al. Characterization of spike glycoprotein of SARS-CoV-2 on virus entry and its immune cross-reactivity with SARS-CoV. Nat Commun. 2020;11:1620. https://doi.org/10.1038/s41467-020-15562-9.
29. Hoffmann M, et al. SARS-CoV-2 Cell Entry Depends on ACE2 and TMPRSS2 and Is Blocked by a Clinically Proven Protease Inhibitor. Cell. 2020;181:271-280.e278. https://doi.org/10.1016/j.cell.2020.02.052.
30. Benton DJ, et al. Receptor binding and priming of the spike protein of SARS-CoV-2 for membrane fusion. Nature. 2020;588:327–30. https://doi.org/10.1038/s41586-020-2772-0.
31. Gu H, et al. Adaptation of SARS-CoV-2 in BALB/c mice for testing vaccine efficacy. Science (New York, NY). 2020;369:1603–7. https://doi.org/10.1126/science.abc4730.
32. Tamura T, et al. Virological characteristics of the SARS-CoV-2 BA.2.86 variant. Cell Host Microbe. 2024;32:170-180.e112. https://doi.org/10.1016/j.chom.2024.01.001.
33. Dadonaite B, et al. Spike deep mutational scanning helps predict success of SARS-CoV-2 clades. Nature. 2024;631:617–26. https://doi.org/10.1038/s41586-024-07636-1.
34. Collier DA, et al. Sensitivity of SARS-CoV-2 B.1.1.7 to mRNA vaccine-elicited antibodies. Nature. 2021;593:136–41. https://doi.org/10.1038/s41586-021-03412-7.
35. McCallum M, et al. Structural basis of SARS-CoV-2 Omicron immune evasion and receptor engagement. Science (New York, NY). 2022;375:864–8. https://doi.org/10.1126/science.abn8652.
36. Li P, et al. Distinct patterns of SARS-CoV-2 BA.2.87.1 and JN.1 variants in immune evasion, antigenicity, and cell-cell fusion. mBio. 2024;15:e0075124-283. https://doi.org/10.1128/mbio.00751-24.
37. Zhao H, et al. SARS-CoV-2 Omicron variant shows less efficient replication and fusion activity when compared with Delta variant in TMPRSS2-expressed cells. Emerging microbes & infections. 2022;11:277–83. https://doi.org/10.1080/22221751.2021.2023329.
38. Zhang Y, et al. SARS-CoV-2 spike L452R mutation increases Omicron variant fusogenicity and infectivity as well as host glycolysis. Signal Transduct Target Ther. 2022;7:76. https://doi.org/10.1038/s41392-022-00941-z.
39. Saito A, et al. Enhanced fusogenicity and pathogenicity of SARS-CoV-2 Delta P681R mutation. Nature. 2022;602:300–6. https://doi.org/10.1038/s41586-021-04266-9.
40. Zhang J, et al. Membrane fusion and immune evasion by the spike protein of SARS-CoV-2 Delta variant. Science (New York, NY). 2021;374:1353–60. https://doi.org/10.1126/science.abl9463.
41. Wang L, et al. Fusogenicity of SARS-CoV-2 BA.2.86 subvariant and its sensitivity to the prokaryotic recombinant EK1 peptide. Cell Discov. 2024;10:6. https://doi.org/10.1038/s41421-023-00631-2.
42. Liu Y, et al. Lineage-specific pathogenicity, immune evasion, and virological features of SARS-CoV-2 BA.2.86/JN.1 and EG.5.1/HK.3. Nat Commun. 2024;15:8728. https://doi.org/10.1038/s41467-024-53033-7.
43. Zhou T, et al. Structural basis for potent antibody neutralization of SARS-CoV-2 variants including B.1.1.529. Science (New York, NY). 2022;376:eabn8897. https://doi.org/10.1126/science.abn8897.
44. Uriu K, et al. Transmissibility, infectivity, and immune evasion of the SARS-CoV-2 BA.2.86 variant. Lancet Infect Dis. 2023;23:e460–1. https://doi.org/10.1016/s1473-3099(23)00575-3.

Publisher's Note